Dendrobium Mixture Improved Diabetic Nephropathy in db/db Mice by Regulating TGF-β1/Smads Signal Transduction

Yong Chen
Fujian University of Traditional Chinese Medicine https://orcid.org/0000-0002-2841-8965
Xiaohui Lin
Fujian University of Traditional Chinese Medicine
Yanfang Zheng
Fujian University of Traditional Chinese Medicine
Wenzhen Yu
Fujian University of Traditional Chinese Medicine
Fan Lin
Fujian University of Traditional Chinese Medicine
Jieping Zhang (zhangjieping@fjtcm.edu.cn)
Fujian University of Traditional Chinese Medicine https://orcid.org/0000-0002-2087-9708

Research

Keywords: Diabetic nephropathy, Dendrobium mixture, TGF-β1/Smads signaling pathway

Posted Date: February 9th, 2021

DOI: https://doi.org/10.21203/rs.3.rs-177708/v1

Dendrobium mixture improved diabetic nephropathy in *db/db* mice by regulating TGF-β1/Smads signal transduction

Yong Chen[1], Xiaohui Lin[1], Yanfang Zheng[2], Wenzhen Yu[1], Fan Lin[1], and Jieping Zhang[1*]

[1]Institute of Integrated Traditional Chinese and Western Medicine, Fujian University of Traditional Chinese Medicine, Fuzhou 350122, China

[2]Institute of Pharmacy, Fujian University of Traditional Chinese Medicine, Fuzhou 350122, China

Abstract

Background: *Dendrobium* mixture (DMix) is an effective treatment for diabetic nephropathy (DN), but the underlying molecular mechanism remains unclear. In this study, we investigated whether DMix regulates the transforming growth factor-β1 (TGF-β1)/Smads signal transduction pathway.

Methods: Twenty-four *db/db* mice were randomly divided into three groups: the model, DMix, and gliquidone groups, while eight *db/m* mice were selected as the normal control group. The drug was administered by continuous gavage for 8 weeks. Body weight (BW), kidney weight (KW), kidney index, fasting blood glucose (FBG), blood lipid, 24-hour urinary

* Correspondence: zhangjieping@fjtcm.edu.cn

[1]Institute of Integrated Traditional Chinese and Western Medicine, Fujian University of Traditional Chinese Medicine, Fuzhou 350122, People's Republic of China

Full list of author information is available at the end of the article

albumin excretion rate, blood urea nitrogen, and serum creatinine levels were measured. Pathological changes in the renal tissue were observed using a light microscope. Real-time quantitative PCR and immunohistochemical staining were used to detect mRNA expression of TGF-β1 and alpha-smooth muscle actin (α-SMA) genes and proteins, respectively, in renal tissues. TGF-β1, Smad2, p-Smad2, Smad3, p-Smad3, and α-SMA expression levels were measured using western blotting.

Results: DMix significantly reduced FBG level, BW, KW, and blood lipid level, and improved renal function in *db/db* mice. Histopathology showed that DMix alleviated glomerular mesangial cell proliferation and renal interstitial fibrosis in *db/db* mice. Additionally, DMix reduced protein and mRNA expression of TGF-β1 and α-SMA, and inhibited Smad2 and Smad3 phosphorylation.

Conclusions: The findings suggest that DMix may inhibit renal fibrosis and delay the progression of DN by regulating the TGF-β1/Smads signaling pathway.

Key words: Diabetic nephropathy, Dendrobium mixture, TGF-β1/Smads signaling pathway

Background

Diabetic nephropathy (DN) is a common chronic microvascular complication of diabetes and the most important cause of death in patients with diabetes [1, 2]. DN is characterized by the thickening of the glomerular basement membrane, proliferation of mesangial cells, and accumulation of extracellular matrix, leading to glomerulosclerosis and interstitial fibrosis [3,4]. Transforming growth factor-β1 (TGF-β1) is a key cytokine-promoting fibrosis, and the Smad protein is the intracellular kinase substrate of the TGF-β1 receptor, mediating the TGF-

β1 signaling pathway. Activation of the TGF-β1/Smads signal transduction pathway is an important mechanism for the development of renal fibrosis [5-7]. *Dendrobium* mixture (DMix) is a preparation used at the Second Affiliated Hospital of Fujian Traditional Chinese Medical University (batch number: Min Q/YZ-2012-315; patent number: ZL201110408411.0) that was developed by Professor Shi Hongfor the long-term clinical treatment of diabetes and its complications. It is composed of *Dendrobium*, *Astragalus*, *Salvia miltiorrhiza*, *Rhizoma anemarrhenae*, and other herbs. It has the effects of lowering glucose and lipid levels and improving insulin resistance following clinical application [8-10], but the potential molecular mechanism remains unclear. In this study, the effect of DMix on the TGF-β1/Smads signaling pathway in the renal tissue of *db/db* mice with DN was observed, and the mechanism by which it improves DN was discussed to provide an experimental basis for the use of DMix in clinical practice.

Methods

Drugs

DMix decoction, consisting of 15 g *Dendrobium*, 20 g *Astragalus,* 8 g *Schisandra*, 15 g *Radix puerariae*, 20 g *Salvia miltiorrhiza*, 18 g *Rehmanniae*, and 12 g *Rhizoma anemarrhenae*, was purchased from Guoyitang Clinic, Fujian University of Traditional Chinese Medicine (FJTCM). Gliquidone tablets (batch no. 1140573) were purchased from Beijing WanhuiShuanghe Pharmaceutical Co., Ltd, Beijing, China.

Animals

db/db Mice (male, 11 weeks old, weight 42-46 g) and *db/m* mice (male, 11 weeks old, weight 21-24 g) were provided by the Department of Experimental Animal Science, Beijing University Medical Science Department (license number: SCXK (Jing) 2011-0012) and kept

in a specific-pathogen-free environment at the Experimental Animal Center, FJTCM, with free access to standard diet and water. All animal experiments were conducted in accordance with internationally recognized animal welfare guidelines and approved by the medical ethics committee of FJTCM.

Experimental procedures

After 1 week of adaptive feeding, according to fasting blood glucose (FBG) level and body weight (BW), *db/db* mice were randomly divided into three groups (n=8): the model group, the DMix group, and the gliquidone group (positive control). In addition, eight *db/m* mice of the same age with normal performance were selected as the normal control group. Mice in the normal control and model groups were administered 20 mL**/**(kg·d) normal saline, the positive control group received 5 mg**/**(kg·d) gliquidone, and the DMix treatment group received 12 g**/**(kg·d) DMix, once a day for 8 weeks.

Biochemical analysis

The FBG level of the mice was measured with a blood glucose meter and a test paper once every 2 weeks during treatment, using blood collected at the tail tip. After 8 weeks of administration, the weight of the mice was determined, and the mice were placed into a metabolic cage. Urine was collected for 24 hours and the urinary albumin excretion rate (UAER) was determined using a urine protein quantitative kit (Nanjing Jiancheng Bioengineering Institute, Nanjing, China). After treatment, all mice were anesthetized via an intraperitoneal injection of 2% sodium pentobarbital (0.01 mL/g). Orbital blood was collected to separate the serum for the detection of blood urea nitrogen (BUN), serum creatinine (Scr), total cholesterol (TC), and triglyceride (TG) levels. All biochemical analysis kits were purchased from Nanjing Jiancheng Bioengineering Institute (Nanjing, China). At the end of

the experiments, the mice were sacrificed by cervical dislocation and kidneys were excised, washed with normal saline, and weighed.

Renal histological analysis

A part of the kidney tissue was fixed in 4% paraformaldehyde solution, embedded in paraffin, cut into 4-μm-thick sections, and then stained with hematoxylin-eosin (HE), periodic Acid-Schiff (PAS), and Masson. The stained kidney sections were examined under a light microscope at a magnification of ×400.

HE staining

The dried kidney tissue sections were dewaxed using xylene, graded alcohol, and distilled water, then stained with hematoxylin for 10 min, differentiated with 1% hydrochloric acid alcohol for 5s, and then put into eosin for 3 min. Then, dehydration and transparent sealing were performed before observation under a light microscope.

PAS staining

The dried kidney tissue sections were dewaxed using xylene, graded alcohol, and distilled water, followed by iodic acid oxidation solution for 5 min and Schiff reagent for 15 min. After hematoxylin staining for 1 min, 1% hydrochloric acid alcohol differentiation for 3 s, dehydration, and transparent sealing were performed for microscopic examination.

Masson staining

Dried kidney tissue sections were dewaxed using xylene, gradient alcohol, and distilled water, and then fixed for 1 h in Bouin fixative solution. Masson composite dyeing solution was soaked for 10 min, and the 1% phosphomolybdate was separated for 10min. The collagen

fiber showed a reddish color and was soaked in 2% aniline blue solution for 5 min. Then, dehydration and transparent sealing were performed before observation under a light microscope.

Real-time quantitative PCR (RT-qPCR)

Total RNA was extracted from mice kidney tissue with RNAiso Plus reagent (Takara, Tokyo, Japan), and the concentration was determined. Then, cDNA was synthesized by reverse transcription using a reverse transcription kit (Takara, Tokyo, Japan). The PCR reaction was performed using a PCR kit (Takara, Tokyo, Japan) under the following reaction conditions: denaturation, 95 °C for 30 s; annealing, 55 °C for 30 s; extension, 72 °C for 1 min; 30 cycles. SDS 2.4 software was used to analyze the CT values of the samples detected during the PCR process, using β-actin as the internal referenceand adopting the ΔΔCt method for relative quantitative analysis, with $2^{-\Delta\Delta Ct}$ as a quantity relative expression of the target RNA. PCR primers (Table 1) were designed and provided by Fuzhou Shangya Biotechnology Co., Ltd (Fuzhou, China).

Table1: RT-qPCR primers

Gene Name	Primer Sequence	Product Length(bp)
TGF-β1	Forward: 5'-CCAGATCCTGTCCAAACTAAGG-3' Reverse: 5'-CTCTTTAGCATAGTAGTCCGCT-3'	169
α-SMA	Forward: 5'-GGACGTACAACTGGTATTGTGC-3' Reverse: 5'-TCGGCAGTAGTCACGAAGGA-3'	179
β-actin	Forward: 5'-GTGACGTTGACATCCGTAAAGA-3' Reverse: 5'-GCCGGACTCATCGTACTCC-3'	245

Immunohistochemistry

The kidney tissue was fixed in 4% paraformaldehyde solution, embedded in paraffin, cut into 4-μm-thick slices, baked for 2 h, dewaxed using xylene twice, hydrated with gradient alcohol, placedinto boiled sodium citrate solution for antigen repair, and cooled naturally to room temperature (18–30 °C). The sections were rinsed with phosphate-buffered saline (PBS) thrice, co-incubated with an endogenous peroxidase blocker at room temperature for 10 min, rinsed with PBS thrice, and co-incubated with non-immunized animal serum at room temperature for 10 min. After removing the serum, primary antibodies were added drop-wise as follows: rabbit anti-TGF-β1 and anti-α-SMA polyclonal antibodies (1:100 dilution each, Abcam, Cambridge, UK), incubated at 4 °C overnight, and rinsed with PBS thrice; biotin-labeled sheep anti-rabbit IgG (ready to use, Fuzhou Maixin BiotechCo., Ltd, Fuzhou, China), incubated at room temperature for 10 min, and rinsed with PBS thrice; streptavidin-peroxidase (Fuzhou Maixin BiotechCo., Ltd, Fuzhou, China), incubated at room temperature for 10 min, and rinsed with PBS thrice. Then, DAB (Wuhan Boster Biological Technology Co., Ltd, Wuhan, China) was added for color development, rinsed with distilled water, hematoxylin-dyed, and tap water-rinsed for blueness. The gradient alcohol was dehydrated and dried, xylene was transparent, neutral gum was sealed, and tan was positively expressed under the optical microscope. The Image-pro Plus 6.0 Image analysis software was used for semi-quantitative analysis, and the relative protein expression was represented by the mean density.

Western blot assays

Kidney tissues stored in liquid nitrogen mixed with appropriate protein lysate were fully ground to produce tissue homogenate. After centrifugation (4 °C, 12,000 rpm, 15 min), the total protein was extracted from the supernatant and the protein concentration was

147 determined using the bicinchoninic acid assay. Then, 30μg of each sample was used for 10%
148 SDS-PAGE gel electrophoresis, transferred to a polyvinylidene fluoride membrane, and
149 sealed with 5% skim milk at room temperature for 1 h. Primary antibodies (TGF-β1, Smad2,
150 p-Smad2, Smad3, p-Smad3, α-SMA) were added and incubated with the membrane overnight
151 at 4 °C. After rinsing with tris-buffered saline, 0.1% Tween 20 (TBST), the membrane was
152 incubated with the secondary antibody at room temperature for 1 h. After TBST rinsing, the
153 membrane was stained using enhanced chemiluminescence and viewed using a gel imaging
154 system. The corresponding antibody dilutions were as follows: β-actin (1:1000 dilution,
155 Abcam, Cambridge, UK), TGF-β1 (1:125 dilution, Abcam, Cambridge, UK), Smad2 (1:1000
156 dilution, Abcam, Cambridge, UK), p-Smad2 (1:300 dilution, Abcam, Cambridge, UK),
157 Smad3 (1:5000 dilution, Abcam, Cambridge, UK), p-Smad3 (1:2000 dilution, Abcam,
158 Cambridge, UK), α-SMA (1:500 dilution, Abcam, Cambridge, UK), goat-anti-mouse IgG
159 secondary antibody (1:2000 dilution, Beyotime, Shanghai, China), goat-anti-rabbit IgG
160 secondary antibody (1:1000 dilution, Beyotime, Shanghai, China). The gray value of the strip
161 was measured using the Image Lab analysis software, and the results are expressed in terms
162 of the relative expression of the target protein, using β-actin as the internal reference.

163 **Statistical analyses**

164 SPSS 22.0 statistical software was used to analyze the data, which are expressed as mean ±
165 standard deviation (SD). Differences among multiple sample groups were analyzed using
166 one-way ANOVA. The Bonferroni method was used for pairwise comparison between
167 groups when the variances were homogeneous, and Tamhane's T2 comparison was used
168 when the variances were heterogeneous. $P<0.05$ was considered statistically significant.

169 ## Results

Comparison of general signs

Mice in the normal group were in a good mental state, responsive, with shiny hair, and in a good feeding condition. *db/db* Mice were listless and unresponsive, with increased diet and urine volumes; the above symptoms of mice in each treatment group were improved to different degrees compared with the model group.

DMix reduced FBG levels of db/db mice

The FBG level in *db/db* mice was approximately 3× higher than that in the normal group (P<0.01). The FBG level in the DMix group gradually decreased with increasing treatment duration (Fig. 1). After the 4th week, there was a significant reduction in the FBG level in the DMix group compared with the model group (week 4, P<0.05; weeks 6 and 8, P<0.01), and no statistically significant difference was observed between the DMix and positive control groups (P>0.05), indicating that DMix could reduce blood glucose in *db/db* mice.

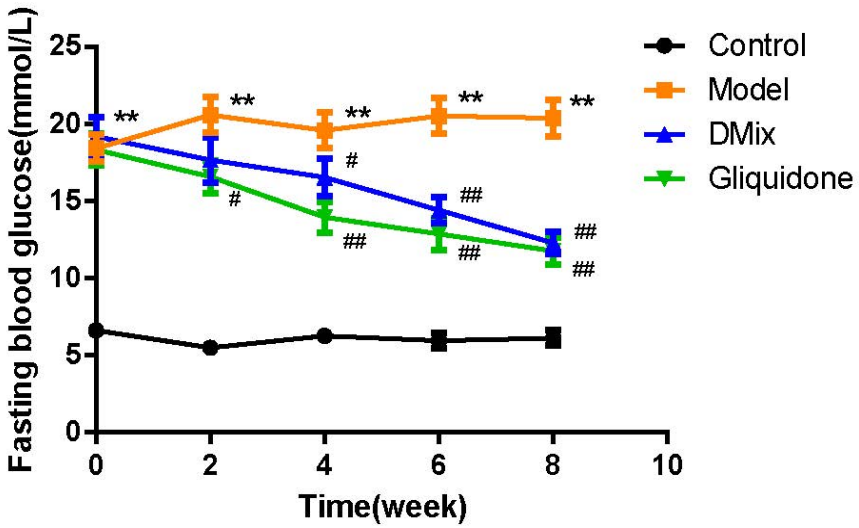

Fig. 1 Eight weeks post-DMix treatment, fasting blood glucose of the normal (Control), model (Model), DMix (DMix), and gliquidone (Gliquidone) groups were tested. Data are presented as mean ± SD of eight animals for each group (n=8). $^{**}P<0.01$ versus Control; $^{\#}P<0.05$ versus Model; $^{\#\#}P<0.01$ versus Model.

Comparison of BW, KW, and KI in each group

The BW, KW, and KI of *db/db* mice were significantly higher than those of the normal group ($P<0.05$, $P<0.01$). After 8 weeks of DMix treatment, the BW, KW, and KI of the mice were all lower than those of the model group to different degrees (KI, $P<0.05$; BW and KI, $P<0.01$) (Fig. 2a-c). Additionally, there was no significant difference between the DMix and gliquidone groups ($P>0.05$).

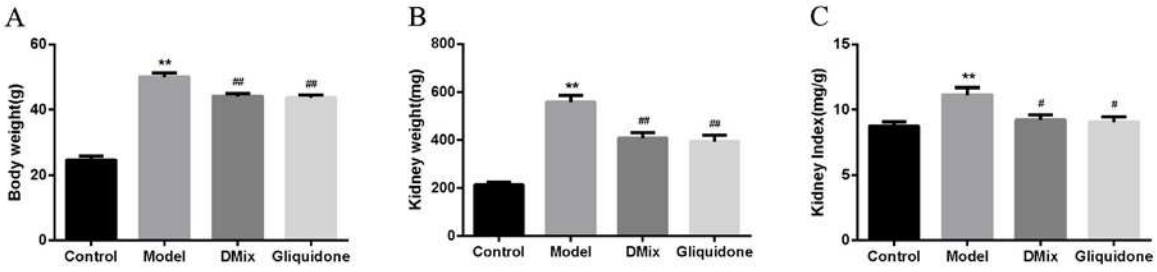

Fig. 2 Changes in body weight (a), kidney weight (b), and kidney index (c) after DMix treatment. Data are presented as mean ± SD from eight animals for each group (n=8). $^{**}P<0.01$ versus Control; $^{\#}P<0.05$ versus Model; $^{\#\#}P<0.01$ versus Model.

Effects of DMix on TC and TG levels in db/db mice

The serum TC and TG levels of mice in the model group were significantly higher than those in the normal group (P<0.01). TC and TG levels in both the Dmix and gliquidone groups were significantly lower than those in the model group (TG, P<0.05; TC, P<0.01) (Fig. 3a, b). There was no significant difference between the Dmix and gliquidone groups (P>0.05). These results indicate that DMix could regulate lipid metabolism.

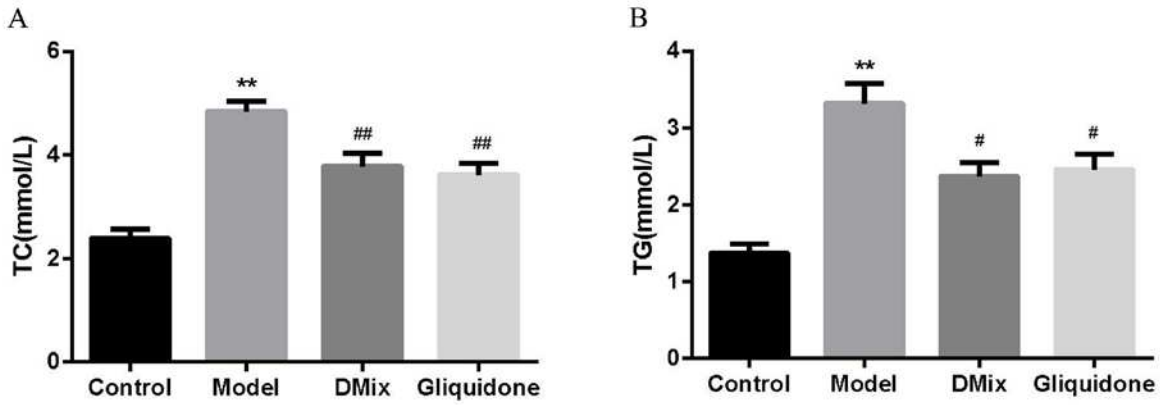

Fig. 3 Values are expressed as mean ± SD of eight samples from each group (n=8). $^{**}P$<0.01 versus Control; $^{\#}P$<0.05 versus Model; $^{\#\#}P$<0.01 versus Model.

DMix improved renal function of db/db mice

Renal function indices of mice in each group were measured, including Scr, BUN, and UAER. These indices were significantly higher in the model group than in the normal group (P<0.01), indicating that the DN mouse model was successfully established and renal insufficiency was achieved in the DN mice. The Scr, BUN, and UAER levels of mice in the DMix group were significantly lower than those in the model group (P<0.05), but there was

no significant difference between the DMix and gliquidone groups (P>0.05) (Fig. 4a-c). These results indicate that DMix had a protective effect on the kidney of *db/db* mice.

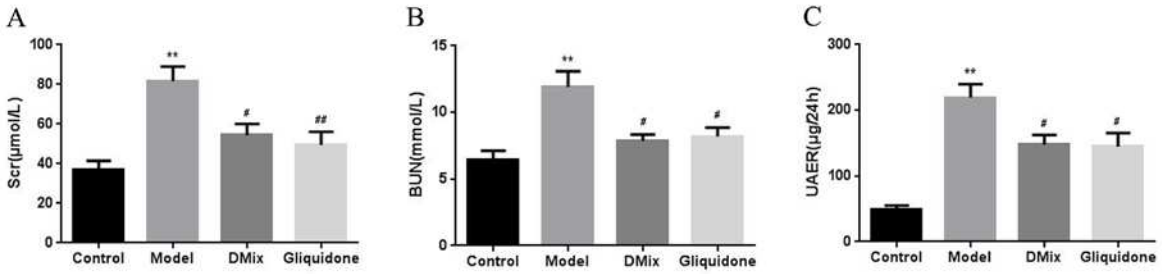

Fig. 4 Values are expressed as mean ± SD of eight samples from each group (n=8). $^{**}P$<0.01 versus Control; $^{\#}P$<0.05 versus Model; $^{\#\#}P$<0.01 versus Model.

Effect of DMix on renal pathological morphology of db/db mice

HE (Fig. 5a) and PAS (Fig. 5b) staining showed clear renal tissue structure, normal glomerular size, morphology, and interstitial space, no increase in mesangial matrix size, unobstructed renal tubular lumen, intact epithelial cells, and no glycogen deposition. *db/db* Mice had glomerular hypertrophy, a larger mesangial matrix, a wider mesangial region, partial capillary lumen stenosis, vacuolar degeneration of renal tubular epithelial cells, more renal mesenchymal cells, and large amounts of red-stained glycogen deposition. Both the DMix and gliquidone groups improved compared to the model group, with thinner glomerular basement membranes, significantly less mesangial cell proliferation, smaller extracellular matrix, and less glycogen deposition than in the model group. Additionally, in the DMix and gliquidone groups, the tubular structure of the kidney was nearly restored to normal. Masson staining (Fig. 5c) showed collagen fiber accumulation in the glomerular and

tubulointerstitial lesions of mice in the model group, and collagen fiber deposition improved significantly after DMix treatment.

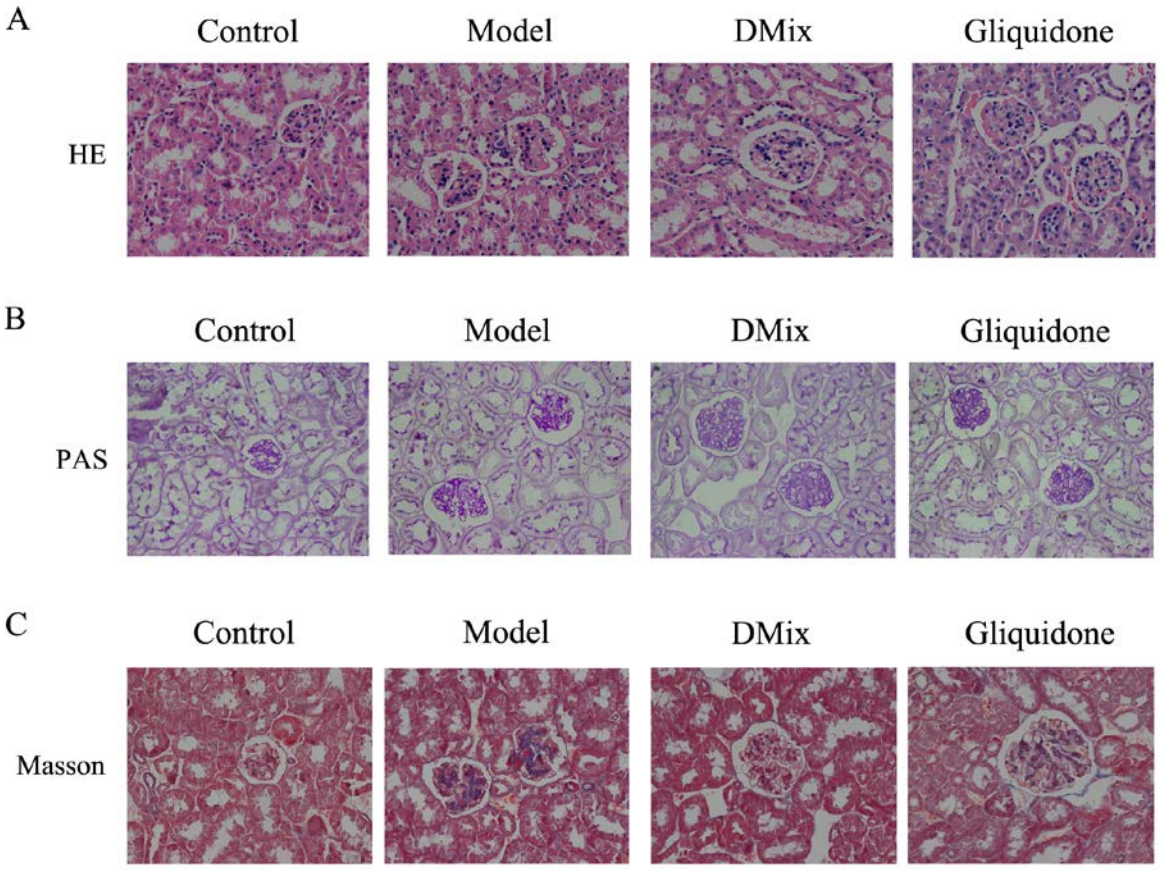

Fig. 5 Photomicrographs of HE (a), PAS (b), and Masson (c) staining of mice kidneys from each group as observed under a light microscope (×400). The kidney specimen of the model group showed markedly severe destruction in glomerular and tubulointerstitial lesions, such as glomerular hypertrophy, increased mesangial matrix, interstitial cell infiltration, and collagen fiber deposition. After treatment, the overall morphology of glomerular and tubulointerstitial lesions improved significantly.

DMix inhibited mRNA expression of TGF-β1 and α-SMA in the renal tissues of db/db mice

TGF-β1 has been identified as a potential target for DN therapy, and the levels of α-SMA, a marker participating in the renal tubular epithelial–mesenchymal transition (EMT) process, is thought to reflect the degree of renal fibrosis [11, 12]. To evaluate the therapeutic effect of DMix, the mRNA expression levels of TGF-β1 and α-SMA in renal tissues were measured using RT-qPCR. The mRNA expression levels of TGF-β1 and α-SMA in renal tissues of mice in the model group were significantly higher than those in the normal group (P<0.01). Moreover, the mRNA expression levels of TGF-β1 and α-SMA in the DMix and gliquidone groups were lower than those in the model group to varying degrees (α-SMA, P<0.05; TGF-β1, P<0.01), but remained higher than the levels in the normal group (Fig. 6). There was no significant difference between the DMix and gliquidone groups (P>0.05), indicating that DMix inhibited the mRNA expression of TGF-β1 and α-SMA in renal tissues of *db/db* mice.

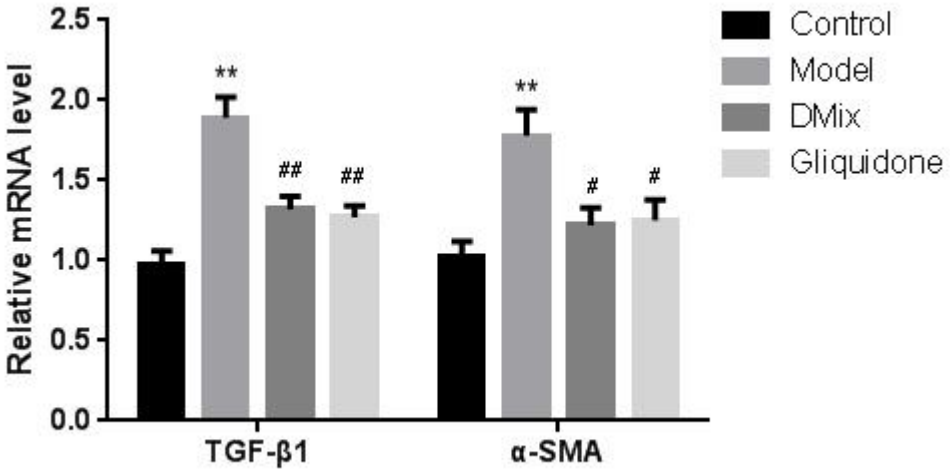

Fig. 6 DMix suppressed the mRNA expression of TGF-β1 and α-SMA in mice kidneys. mRNA levels of TGF-β1 and α-SMA were determined using RT-qPCR, using β-actin as the internal standard for each sample. Data for relative quantity of TGF-β1 and α-SMA mRNA after analysis. $^{**}P<0.01$ versus Control; $^{\#}P<0.05$ versus Model; $^{\#\#}P<0.01$ versus Model.

DMix inhibited the expression of TGF-β1 and α-SMA proteins in the renal tissues of db/db mice

To further demonstrate the therapeutic effect of DMix, immunohistochemical staining was used to detect the expression of TGF-β1 and α-SMA proteins in the renal tissues of mice. The results were consistent with those of RT-qPCR. TGF-β1 and α-SMA were weakly expressed in the kidneys of mice in the normal group, but strongly expressed in the model group (TGF-β1, $P<0.05$; α-SMA, $P<0.01$). The protein expression of TGF-β1 and α-SMA was significantly lower in both treatment groups than in the model group ($P<0.05$), but remained higher than that in the normal group (Fig. 7a-c). There was no significant difference between the DMix and gliquidone groups ($P>0.05$), indicating that DMix inhibited the expression of TGF-β1 and α-SMA proteins in the renal tissues of *db/db* mice.

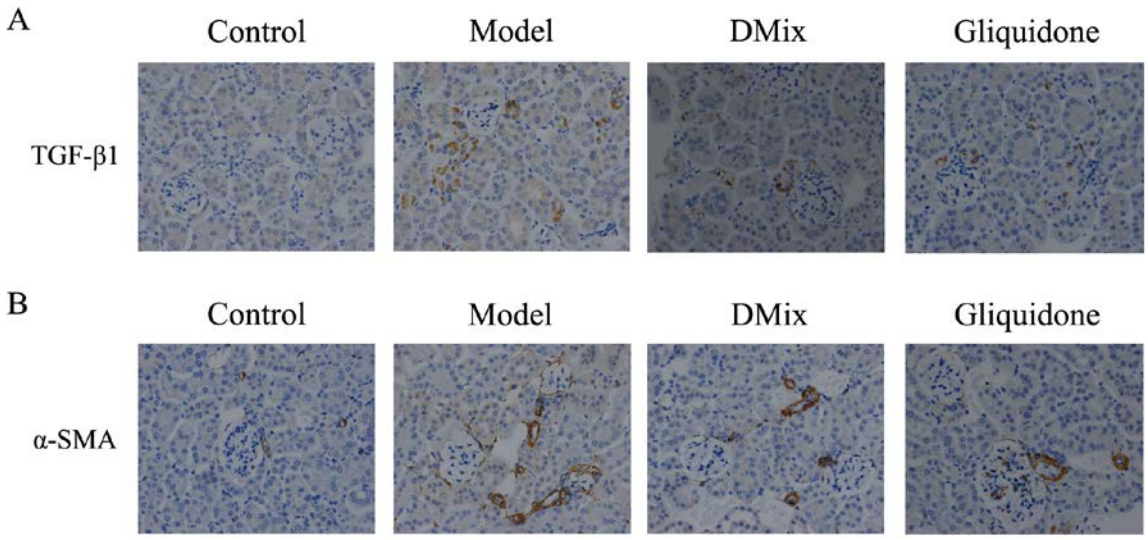

280

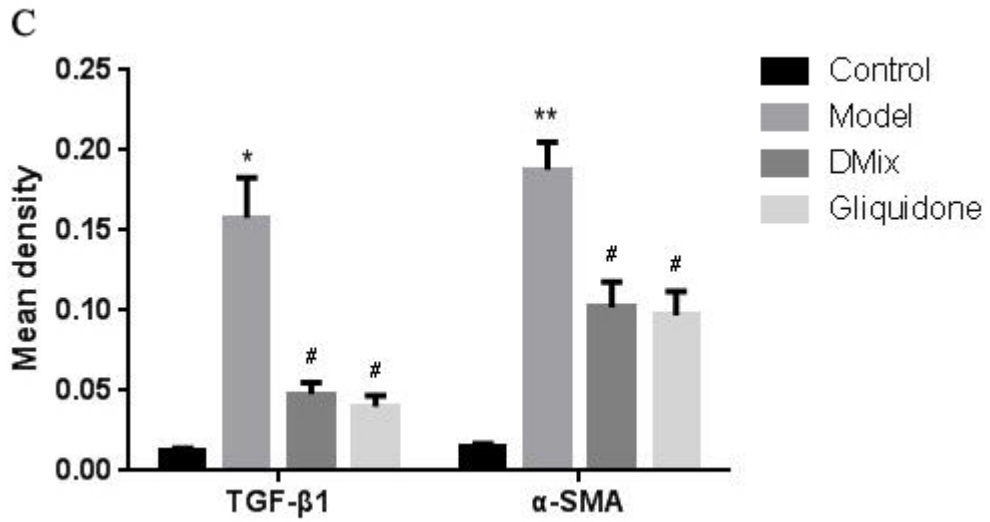

281

282 **Fig. 7** DMix suppressed the expression of TGF-β1 (a) and α-SMA (b) proteins in the kidney,
283 as observed via immunohistochemical analysis under a light microscope (×400). (c) $^{*}P<0.05$
284 versus Control; $^{**}P<0.01$ versus Control; $^{\#}P<0.05$ versus Model.

285

286 **DMix inhibited the TGF-β1/Smads signaling pathway in the renal tissues of db/db mice**

The activation of the Smad pathway and its subsequent nuclear transposition are key steps in TGF-β1-mediated renal fibrosis in DN [13]. The phosphorylation of Smad2 and Smad3 is also an important signal transduction process in the TGF-β1/Smads signaling pathway, and their expression indicates TGF-β1/Smads signaling pathway activation [14]. The expression of TGF-β1, Smad2, p-Smad2, Smad3, p-Smad3, and α-SMA in mouse renal tissues was measured via western blotting. The protein expression of TGF-β1, p-Smad2, p-Smad3, and α-SMA in the model group was significantly higher than that in the normal group (P<0.01), indicating that the TGF-β1/Smads signaling pathway was activated in *db/db* mouse renal tissue. After 8 weeks of treatment with DMix, the expression of TGF-β1, p-Smad2, p-Smad3, and α-SMA proteins was significantly lower than that in the model group (TGF-β1:β-actin, p-Smad2:Smad2, and α-SMA:β-actin, P<0.05; p-Smad3:Smad3, P<0.01), but there was no significant change in the expression of the Smad2 and Smad3 proteins (Fig. 8a-d). There was no significant difference between the DMix and gliquidone groups (P>0.05). Western blots show that DMix inhibited the TGF-β1/Smads signaling pathway in the renal tissues of *db/db* mice.

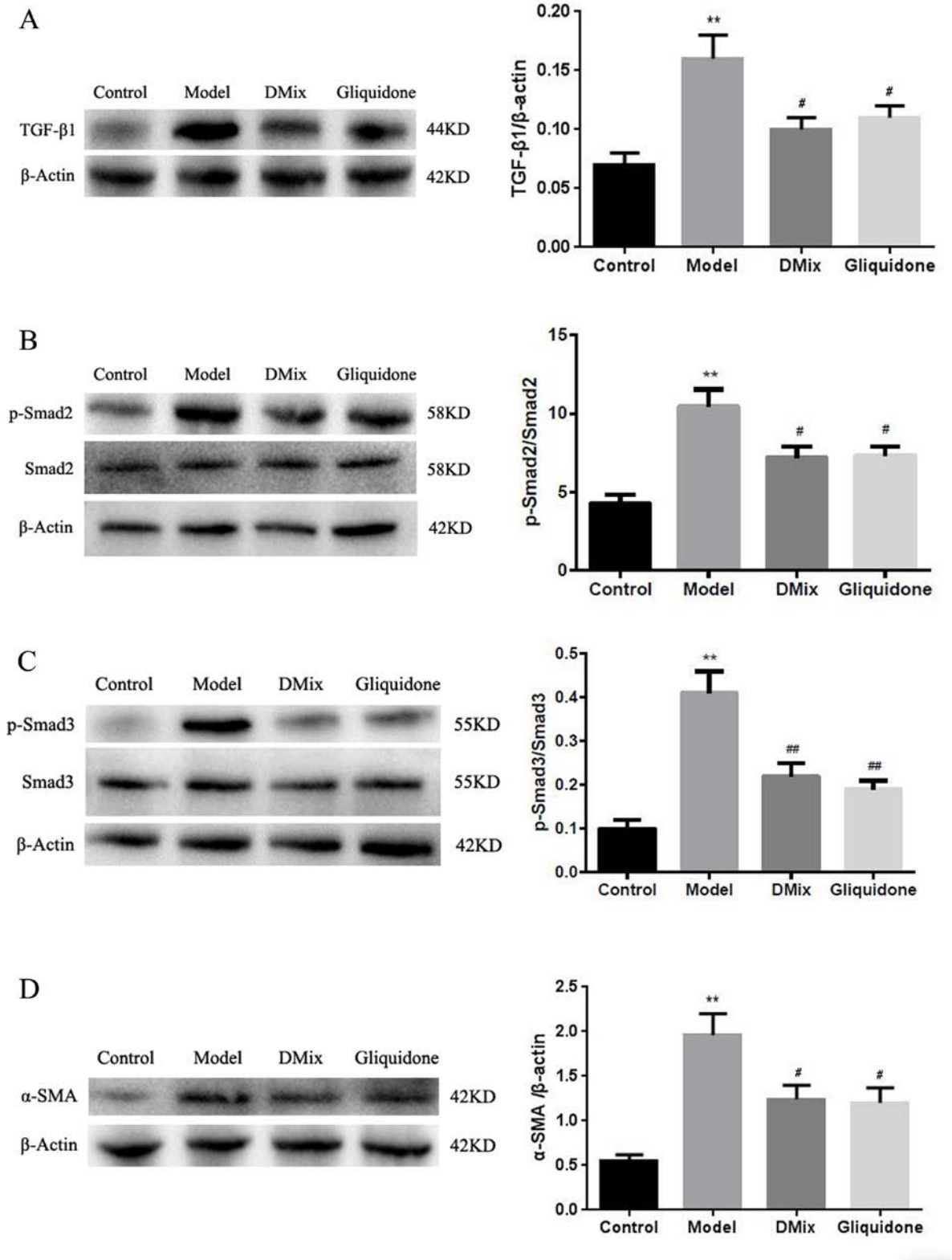

303

304 **Fig. 8** DMix inhibits the renal TGF-β1/Smads signaling pathway in *db/db* mice, as shown
305 using western blotting. β-Actin, Smad2, and Smad3 were used as internal standards. The
306 relative expression were the ratios of TGF-β1:β-actin (a), p-Smad2:Smad2 (b), p-

Smad3:Smad3 (c), and α-SMA:β-actin (d) determined via densitometric analysis. $^{**}P<0.01$ versus Control; $^{\#}P<0.05$ versus Model; $^{\#\#}P<0.01$ versus Model.

Discussion

Currently, DN poses a great threat to human health, and traditional Chinese medicine has achieved good efficacy in the treatment of DN. In preliminary experimental studies and clinical practice, DMix has been shown to have a good therapeutic effect on diabetes mellitus and its complications [15-17, 8-10]. In this study, we observed that DMix can treat DN by inhibiting renal fibrosis and improving renal function. DMix reduced the expression of TGF-β1 and α-SMA, inhibited the phosphorylation of Smad2 and Smad3, thereby slowing DN progression.

DN is caused by a variety of factors, including hyperglycemia, hypertension, and hyperlipidemia [18-20]. The *db/db* mouse is a widely used animal model for the study of DN, and the pathogenesis is caused by a deficiency of the leptin receptor gene [21, 22].The results of this experiment showed that *db/db* mice had a significantly greater body weight than *db/m* mice. Additionally, blood glucose, Scr and BUN levels, and KI were significantly higher in *db/db* mice than in the normal group. Furthermore, the *db/db* mice exhibited proteinuria, dyslipidemia, glomerular hypertrophy, and fibrosis, confirming that the DN model was successful. After treatment with DMix, these parameters were significantly attenuated (Fig. 1-4), which was consistent with previous studies and our clinical observation [9-11]. Additionally, HE, PAS, and Masson staining showed that the degree of renal pathological injury and fibrous hyperplasia improved significantly in the model group with the administration of DMix (Fig. 5). DN is characterized by proteinuria and glomerular sclerosis

330 [23, 24], and our results indicate that DMix not only reduces urinary protein levels, but also
331 reduces renal fibrosis, suggesting that DMix effectively prevents the development of DN.

332 The pathogenesis of DN is complex and has not been fully elucidated. Renal interstitial
333 fibrosis is an important mechanism of renal deterioration in the pathogenesis of DN.
334 Therefore, the key to delay the development of DN is to inhibit renal interstitial fibrosis
335 [25,26]. TGF-β1/Smads is the core pathway of renal fibrosis and one of the important factors
336 in the development of DN [27, 28]. TGF-β1 is considered an important factor contributing to
337 renal mesenchymal fibrosis, and previous studies have confirmed that TGF-β1 is over
338 expressed in DN [29, 30]. Smad2 and Smad3 act downstream of TGF-β1, which promotes
339 Smad2 and Smad3 phosphorylation when activated. Both proteins, which have a high
340 homology, are subsequently transferred to the nucleus, and regulate the expression of
341 fibrosis-related target genes, such as α-SMA, to accelerate the progression of fibrosis [31-33].
342 The expression of p-Smad2 and p-Smad3 proteins is a marker of TGF-β1/Smads signaling
343 pathway activation [34, 35]. Studies have shown that p-Smad2 and p-Smad3 expression
344 levels increase significantly in patients with chronic kidney disease and animal models of
345 renal fibrosis, thereby activating the TGF-β1/Smads signaling pathway and simultaneously
346 increasing the expression of α-SMA protein, a marker of mesenchymal cells, the expression
347 level of which reflects the degree of renal fibrosis [36-38]. The inhibition of the TGF-
348 β1/Smads signaling pathway can effectively reduce DN renal fibrosis and improve renal
349 function [39, 40]. In this study, immunohistochemical (Fig. 7) and western blot (Fig. 8)
350 analyses showed that the expression levels of TGF-β1, p-Smad2, p-Smad3, and α-SMA
351 proteins decreased significantly in the DMix group. The mRNA expression of TGF-β1 and α-
352 SMA (Fig. 6) was consistent with the protein expression of TGF-β1 and α-SMA. These
353 results suggest that DMix may inhibit renal fibrosis owing to DN by negatively regulating the
354 TGF-β1/Smads pathway.

Although the results confirmed our hypothesis, our study may have had some limitations. For example, although DMix had an effect on DN renal fibrosis, more and larger studies and clinical trials are needed for further verification. Additionally, owing to time and financial constraints, we could not carry out cellular experiments to investigate the effect of DMix on DN, and the specific mechanism still needs to be studied.

Conclusion

Our results show that DMix has a protective effect on the kidneys of DN mice, which may be to inhibit renal EMT and fibrosis by regulating the TGF-β1/Smads pathway, thereby delaying the progression of DN. Therefore, DMix may be a promising drug for DN treatment.

Abbreviations

TGF-β1: Transforming growth factor-β1; α-SMA: Alpha-smooth muscle actin; DN: Diabetic nephropathy; BW: Body weight; KW: kidney weight; KI: kidney index; FBG: Fasting blood glucose; UAER: urinary albumin excretion rate; BUN: Blood urea nitrogen; Scr: Serum creatinine; TC: total cholesterol; TG: triglyceride; FJTCM: Fujian University of Traditional Chinese Medicine; HE: Hematoxylin-eosin; PAS: Periodic Acid-Schiff; RT-qPCR: Real-time quantitative PCR; PBS: Phosphate-buffered saline; EMT: Epithelial–mesenchymal transition; DMix: Dendrobium mixture

Acknowledgements

We would like to thank Fujian University of Traditional Chinese Medicine Laboratory Animal Center for providing the laboratory.

Authors' contributions

YC, XHL, YFZ and JPZ participated in the study design. YC, XHL, YFZ and WZY performed the experiments. YC, XHL, YFZ, WZY, FL and JPZ performed the data analysis. YC wrote and JPZ reviewed the manuscript. All authors have read and approved the final manuscript.

Funding

This work was supported by the Fujian University of Traditional Chinese Medicine's research platform management project [No. X2019001-platform], the Natural Science Foundation of Fujian Province [No. 2018J01873, No. 2019J01333], and the National Natural Science Foundation of China [No. 81703909].

Availability of data and materials

The datasets analyzed during the current study are available from the corresponding author on reasonable request.

Ethics approval

The present study was carried out in accordance with the recommendations of the Guidelines for the Care and Use of Laboratory Animals of the Ministry of Science and Technology of China. The protocol was approved by the Medical Ethics Committee of Fujian University of Traditional Chinese Medicine.

Consent for publication

Not applicable.

Competing interests

The authors declare that they have no competing interests.

Author details

[1]Institute of Integrated Traditional Chinese and Western Medicine, Fujian University of Traditional Chinese Medicine, Fuzhou 350122, People's Republic of China. [2]Institute of Pharmacy, Fujian University of Traditional Chinese Medicine, Fuzhou 350122, People's Republic of China.

References

[1] Yabing Xiong, Lili Zhou. The signaling of cellular senescence in diabetic nephropathy. Oxid Med Cell Longev. 2019;2019:7495629. https://doi.org/10.1155/2019/7495629.

[2] Huan Lian, Yi Cheng, Xiaoyan Wu. TMEM16A exacerbates renal injury by activating P38/JNK signaling pathway to promote podocyte apoptosis in diabetic nephropathy mice. Biochem Biophys Res Commun. 2017;487(2):201-8. https://doi.org/10.1016/j.bbrc.2017.04.021.

[3] Carolina Lavoz, Raul R Rodrigues-Diez, Anita Plaza, Daniel Carpio, Jesús Egido, Marta Ruiz-Ortega, et al. VEGFR2 blockade improves renal damage in an experimental model of type 2 diabetic nephropathy. J Clin Med. 2020;9(2):302. https://doi.org/10.3390/jcm9020302.

[4] Li Li, Xiuhui Zhang, Zhicheng Li, Rui Zhang, Ruikun Guo, Qinghua Yin, et al. Renal pathological implications in type 2 diabetes mellitus patients with renal involvement. J Diabetes Complications. 2017;31(1):114-21. https://doi.org/10.1016/j.jdiacomp.2016.10.024.

[5] Le Wang, Teng Ding, Wei-Ling Gong, Chang-Hua Yang, Feng Liu, et al. Effective components of traditional Chinese medicine for regulating TGF-Beta1/Smads signaling pathway in hepatic fibrosis. Zhongguo Zhong Yao Za Zhi. 2019;44(4):666-74 (in Chinese). https://doi.org/10.19540/j.cnki.cjcmm.20181221.006 PMID: 30989878.

[6] He-He Hu, Dan-Qian Chen, Yan-Ni Wang, Ya-Long Feng, Gang Cao, Nosratola D Vaziri, et al. New insights into TGF-β/Smad signaling in tissue fibrosis. Chem Biol Interact. 2018;292:76-83. https://doi.org/10.1016/j.cbi.2018.07.008.

[7] Kotaro Soji, Shigehiro Doi, Ayumu Nakashima, Kensuke Sasaki, Toshiki Doi, Takao Masaki. Deubiquitinase inhibitor PR-619 reduces Smad4 expression and suppresses renal fibrosis in mice with unilateral ureteral obstruction. PLoS One. 2018;13(8):e0202409. https://doi.org/10.1371/journal.pone.0202409.

[8] Qian Xu, Yun Liu, Yi-Bo Cong, Yuan-Yan Zheng, Jie-Ping Zhang, Yi Cui, et al. Gene expression and microarray investigation of *Dendrobium* mixture as progressive therapy for the treatment of type 2 diabetes mellitus. Tropical Journal of Pharmaceutical Research. 2013;12(2):195-201 (in Nigeria). https://doi.org/10.4314/tjpr.v12i2.10.

[9] Jieping Zhang, Xiaoling Zheng, Jiazhu Hong, Jicheng Chen, Yuanyan Zheng, Jinzhong Xin, et al. 90 cases of type 2 diabetes were treated by compound *Dendrobium* mixture. Journal of Fujian University of Traditional Chinese Medicine. 2011;21(5):6-8 (in Chinese). https://doi.org/10.3969/j.issn.1004-5627.2011.05.003.

[10] Baolian Wang, Xinjun Lin, Shuqin Pang, Lixiu Zheng, Yangyang Mei, Bixiang Xu, et al. Meta-analysis of clinical efficacy of *Dendrobium* mixture in the treatment of type 2 diabetes. Journal of Qiqihar medical college. 2017; 38(9):998-1002 (in Chinese). https://doi.org/10.3969/j.issn.1002-1256.2017.09.003.

[11] Shuo Wang, Yi Zhou, Yue Zhang, Xingyu He, Xiangning Zhao, Hairong Zhao, et al. Roscovitine attenuates renal interstitial fibrosis in diabetic mice through the TGF-β1/p38

MAPK pathway. Biomed Pharmacother. 2019;115:108895. https://doi.org/10.1016/j.biopha.2019.108895.

[12] Fengjuan Huang, Yanyan Zhao, Qingzhu Wang, Jan-Luuk Hillebrands, Jacob van den Born, Linlin Ji, Tingting An, et al. Dapagliflozin attenuates renal tubulointerstitial fibrosis associated with type 1 diabetes by regulating STAT1/TGFβ1 signaling. Front Endocrinol (Lausanne). 2019;10:441. https://doi.org/10.3389/fendo.2019.00441.

[13] Xuemin He, Rui Cheng, Chao Huang, Yusuke Takahashi, Yanhui Yang, Siribhinya Benyajati, et al. A novel role of LRP5 in tubulointerstitial fibrosis through activating TGF-β/Smad signaling. Signal Transduct Target Ther. 2020;5(1):45. https://doi.org/10.1038/s41392-020-0142-x.

[14] Hong Xing Zheng, Shan Shan Qi, Jia He, Ching Yuan Hu, Hao Han, Hai Jiang, et al. Cyanidin-3-glucoside from black rice ameliorates diabetic nephropathy via reducing blood glucose, suppressing oxidative stress and inflammation, and regulating transforming growth factor β1/Smad expression. J Agric Food Chem. 2020;68(15):4399-410. https://doi.org/10.1021/acs.jafc.0c00680.

[15] Xinjun Lin, Hong Shi, Yi Cui, Xiaoning Wang, Jieping Zhang, Wenzhen Yu, et al. *Dendrobium* mixture regulates hepatic gluconeogenesis in diabetic rats via the phosphoinositide-3-kinase/protein kinase B signaling pathway. Exp Ther Med. 2018;16(1):204-12. https://doi.org/10.3892/etm.2018.6194.

[16] Yun Liu, Xinjun Lin, Hong Shi, Qian Xu. Effects of *Dendrobium* mixture on the expression of genes related to lipid metabolism and lipid levels in diabetic rats. Journal of Gansu University of Chinese Medicine. 2019;36(5):1-7 (in Chinese). https://www.cnki.com.cn/Article/CJFDTotal-GSZX201905001.htm.

[17] Lin Wang, Hong Shi, Jieping Zhang, Xuehua Zheng, Xiaoning Wang. Effect of Shihu-Compound on Visfatin and Blood Glucose in Diabetic Rats. Fujian Journal of Traditional

Chinese Medicine. 2019;50(1):39-41 (in Chinese). https://doi.org/10.3969/j.issn.1000-338X.2019.01.013.

[18] Muhammad Maqbool, Mark E Cooper, Karin A M Jandeleit-Dahm. Cardiovascular disease and diabetic kidney disease. Semin Nephrol. 2018;38(3):217-32. https://doi.org/10.1016/j.semnephrol.2018.02.003.

[19] Radia Marium Modhumi Khan, Zoey Jia Yu Chua, Jia Chi Tan, Yingying Yang, Zehuan Liao, Yan Zhao. From pre-diabetes to diabetes: diagnosis, treatments and translational research. Medicina (Kaunas). 2019;55(9):546. https://doi.org/10.3390/medicina55090546.

[20] Myriam Rheinberger, Roland Büttner, Carsten A Böger. New aspects in prevention and therapy of diabetic nephropathy. Dtsch Med Wochenschr. 2016;141(3):186-9. https://doi.org/10.1055/s-0041-109591 PMID: 26841180.

[21] Bingxuan Wang, P Charukeshi Chandrasekera, John J Pippin. Leptin-and leptin receptor-deficient rodent models: relevance for human type 2 diabetes. Curr Diabetes Rev. 2014;10(2):131-45. https://doi.org/10.2174/1573399810666140508121012.

[22] Bin Zhang, Xuelian Zhang, Chenyang Zhang, Qiang Shen, Guibo Sun, Xiaobo Sun. Notoginsenoside R1 protects *db/db* mice against diabetic nephropathy via upregulation of Nrf2-mediated HO-1 expression. Molecules. 2019;24(2):247. https://doi.org/10.3390/molecules24020247.

[23] So Young Kim, Tae Dong Jeong, Woochang Lee, Sail Chun, Sung Sunwoo, Soon Bae Kim, et al. Plasma neutrophil gelatinase-associated lipocalin as a marker of tubular damage in diabetic nephropathy. Ann Lab Med. 2018;38(6):524-9. https://doi.org/10.3343/alm.2018.38.6.524.

[24] Praveen Kumar Etta, M V Rao, S Gowrishankar. Collapsing glomerulopathy superimposed on diabetic nephropathy. Indian J Nephrol. 2019;29(3):207-10.

493 https://doi.org/10.4103/ijn.IJN_334_17.
494 [25] Yujin Ma, Jingxia Shi, Feifei Wang, Shipeng Li, Jie Wang, Chaoxia Zhu, et al. MiR-
495 130b increases fibrosis of HMC cells by regulating the TGF-β1 pathway in diabetic
496 nephropathy. J Cell Biochem. 2019;120(3):4044-56. https://doi.org/10.1002/jcb.27688.
497 [26] Ying Xiao, Xiaohan Jiang, Can Peng, Yingying Zhang, Yawen Xiao, Dan Liang, et al.
498 BMP-7/Smads-induced inhibitor of differentiation 2 (Id2) upregulation and Id2/Twist
499 interaction was involved in attenuating diabetic renal tubulointerstitial fibrosis. Int J
500 Biochem Cell Biol. 2019;116:105613. https://doi.org/10.1016/j.biocel.2019.105613.
501 [27] Jing Liu, Tan Deng, Yaxin Wang, Mengmeng Zhang, Guannan Zhu, Haiming Fang, et al.
502 Calycosin inhibits intestinal fibrosis on CCD-18Co cells via modulating transforming
503 growth factor-β/Smad signaling pathway. Pharmacology. 2019;104(1-2):81-9.
504 https://doi.org/10.1159/000500186.
505 [28] Feng Tian, Zhe Wang, Junqiu He, Zhihao Zhang, Ninghua Tan. 4-Octyl itaconate
506 protects against renal fibrosis via inhibiting TGF-β/Smad pathway, autophagy and
507 reducing generation of reactive oxygen species. Eur J Pharmacol. 2020;873:172989.
508 https://doi.org/10.1016/j.ejphar.2020.172989.
509 [29] Happy Sawires, Osama Botrous, Abdelmegeed Aboulmagd, Nadia Madani, Osama
510 Abdelhaleem. Transforming growth factor-β1 in children with diabetic nephropathy.
511 Pediatric Nephrology. 2019;34(1):81-5. https://doi.org/10.1007/s00467-018-4062-8.
512 [30] Na Du, Zhiping Xu, Mingyue Gao, Peng Liu, Bo Sun, Xia Cao. Combination of
513 ginsenoside Rg1 and astragaloside IV reduces oxidative stress and inhibits TGF-
514 β1/Smads signaling cascade on renal fibrosis in rats with diabetic nephropathy. Drug Des
515 Devel Ther. 2018;12:3517-24. https://doi.org/10.2147/DDDT.S171286.
516 [31] Eun Hye Lee, Kwang-Il Park, Kwang-Youn Kim, Ju-Hee Lee, Eun Jeong Jang, Sae
517 Kwang Ku, et al. Liquiritigenin inhibits hepatic fibrogenesis and TGF-β1/Smad with

518 Hippo/YAP signal. Phytomedicine. 2019;62:152780.
519 https://doi.org/10.1016/j.phymed.2018.12.003.
520 [32] Peng Wang, Man-Li Luo, Erwei Song, Zhanmei Zhou, Tongtong Ma, Jun Wang, et al.
521 Long noncoding RNA lnc-TSI inhibits renal fibrogenesis by negatively regulating the
522 TGF-β/Smad3 pathway. Sci Transl Med. 2018;10(462):eaat2039.
523 https://doi.org/10.1126/scitranslmed.aat2039.
524 [33] Xiaohua Pan, Jiahong Li, Xing Tu, Chengfei Wu, He Liu, Yang Luo, et al. Lysine-
525 specific demethylase-1 regulates fibroblast activation in pulmonary fibrosis via TGF-
526 β1/Smad3 pathway. Pharmacol Res. 2020;152:104592.
527 https://doi.org/10.1016/j.phrs.2019.104592.
528 [34] Ken-Ichi Miyazono, Saho Moriwaki, Tomoko Ito, Akira Kurisaki, Makoto Asashima,
529 Masaru Tanokura. Hydrophobic patches on SMAD2 and SMAD3 determine selective
530 binding to cofactors. Sci Signal. 2018;11(523):eaao7227.
531 https://doi.org/10.1126/scisignal.aao7227.
532 [35] Lirong Liu, Yuanyuan Wang, Rui Yan, Shuang Li, Mingjun Shi, Ying Xiao, et al.
533 Oxymatrine inhibits renal tubular EMT induced by high glucose via upregulation of
534 SnoN and inhibition of TGF-β1/Smad Signaling Pathway. PLoS One. 2016;11(3):
535 e0151986. https://doi.org/10.1371/journal.pone.0151986.
536 [36] Lei Zhang, Changsong Han, Fei Ye, Yan He, Yinji Jin, Tianzhen Wang, et al. Plasma
537 gelsolin induced glomerular fibrosis via the TGF-β1/Smads signal transduction pathway
538 in IgA nephropathy. Int J Mol Sci, 2017;18(2):390.
539 https://doi.org/10.3390/ijms18020390.
540 [37] Yan-Ru Huang, Qing-Xue Wei, Yi-Gang Wan, Wei Sun, Zhi-Min Mao, Hao-Li Chen, et
541 al. Ureic clearance granule, alleviates renal dysfunction and tubulointerstitial fibrosis by
542 promoting extracellular matrix degradation in renal failure rats, compared with enalapril.

J Ethnopharmacol. 2014;155(3):1541-52. https://doi.org/10.1016/j.jep.2014.07.048.

[38] Yaning Wang, Chao Lin, Qiang Ren, Yunqi Liu, Xiangdong Yang. Astragaloside effect on TGF-β1, SMAD2/3, and α-SMA expression in the kidney tissues of diabetic KKAy mice. Int J Clin Exp Pathol. 2015;8(6):6828-34. https://pubmed.ncbi.nlm.nih.gov/26261569 PMID: 26261569; PMCID: PMC4525903.

[39] Lan Yao, Linlin Li, Xinxia Li, Hui Li, Yujie Zhang, Rui Zhang, et al. The anti-inflammatory and antifibrotic effects of Coreopsis tinctoria Nutt on high-glucose-fat diet and streptozotocin-induced diabetic renal damage in rats. BMC Complement Altern Med. 2015;15:314. https://doi.org/10.1186/s12906-015-0826-x.

[40] Fengjuan Tang, Yarong Hao, Xue Zhang, Jian Qin. Effect of echinacoside on kidney fibrosis by inhibition of TGF-β1/Smads signaling pathway in the *db/db* mice model of diabetic nephropathy. Drug Des Devel Ther. 2017;11:2813-26. https://doi.org/10.2147/DDDT.S143805.

Figures

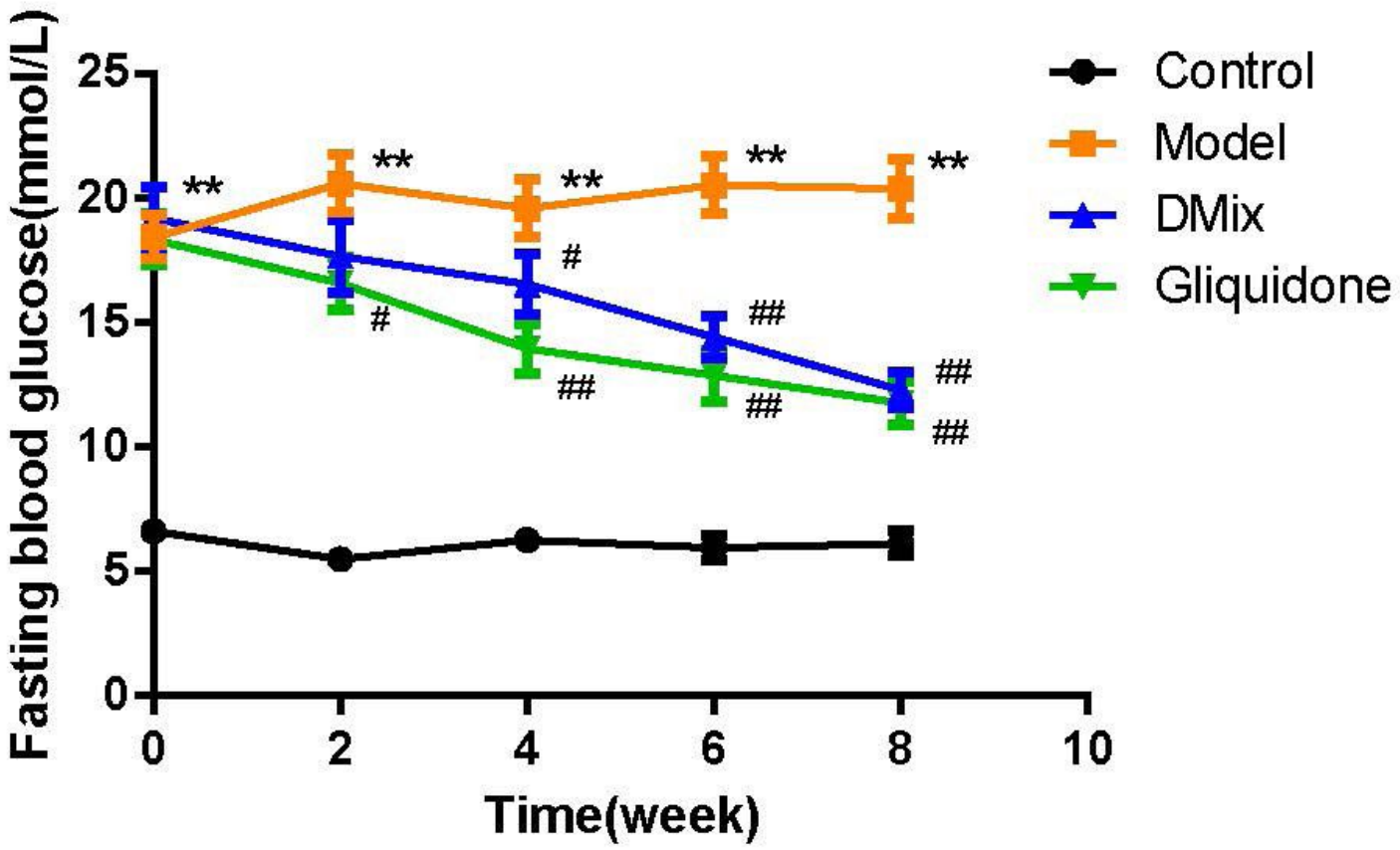

Figure 1

Eight weeks post-DMix treatment, fasting blood glucose of the normal (Control), model (Model), DMix (DMix), and gliquidone (Gliquidone) groups were tested. Data are presented as mean ± SD of eight animals for each group (n=8). **P<0.01 versus Control; #P<0.05 versus Model; ##P<0.01 versus Model.

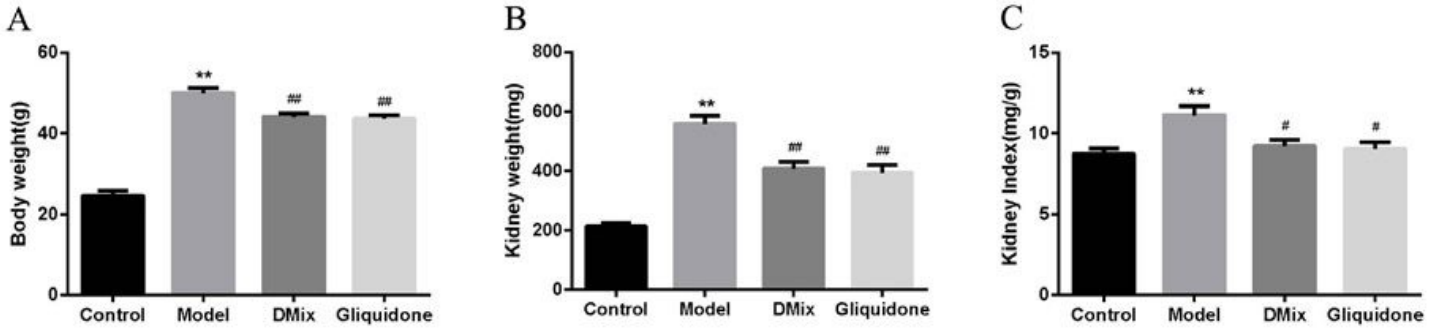

Figure 2

Changes in body weight (a), kidney weight (b), and kidney index (c) after DMix treatment. Data are presented as mean ± SD from eight animals for each group (n=8). **P<0.01 versus Control; #P<0.05

versus Model; ##P<0.01 versus Model.

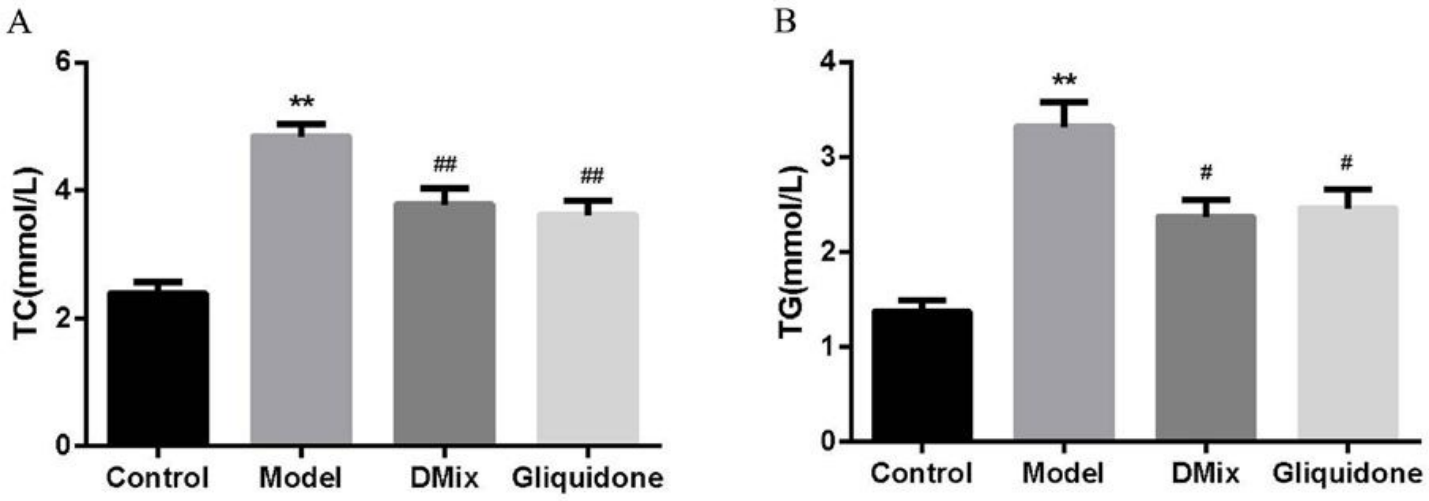

Figure 3

Values are expressed as mean ± SD of eight samples from each group (n=8). **P<0.01 versus Control; #P<0.05 versus Model; ##P<0.01 versus Model.

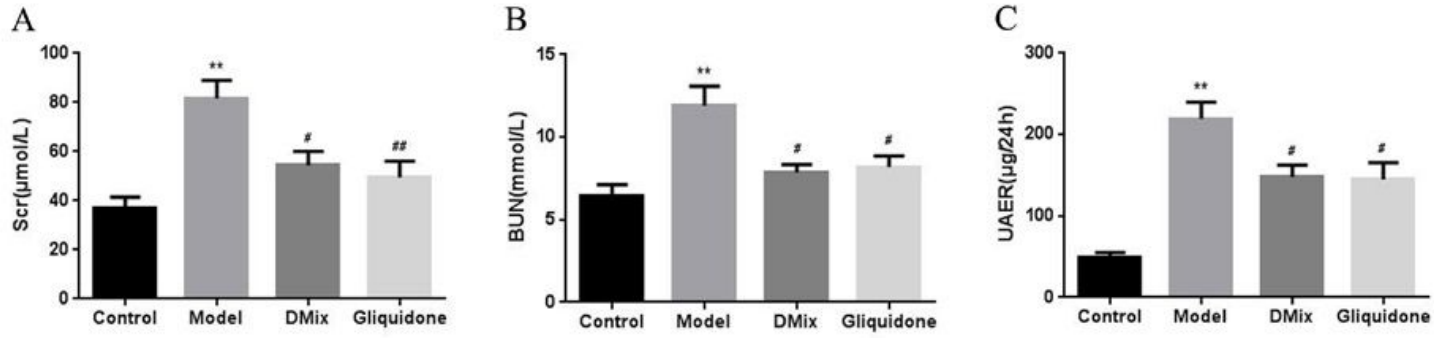

Figure 4

Values are expressed as mean ± SD of eight samples from each group (n=8). **P<0.01 versus Control; #P<0.05 versus Model; ##P<0.01 versus Model.

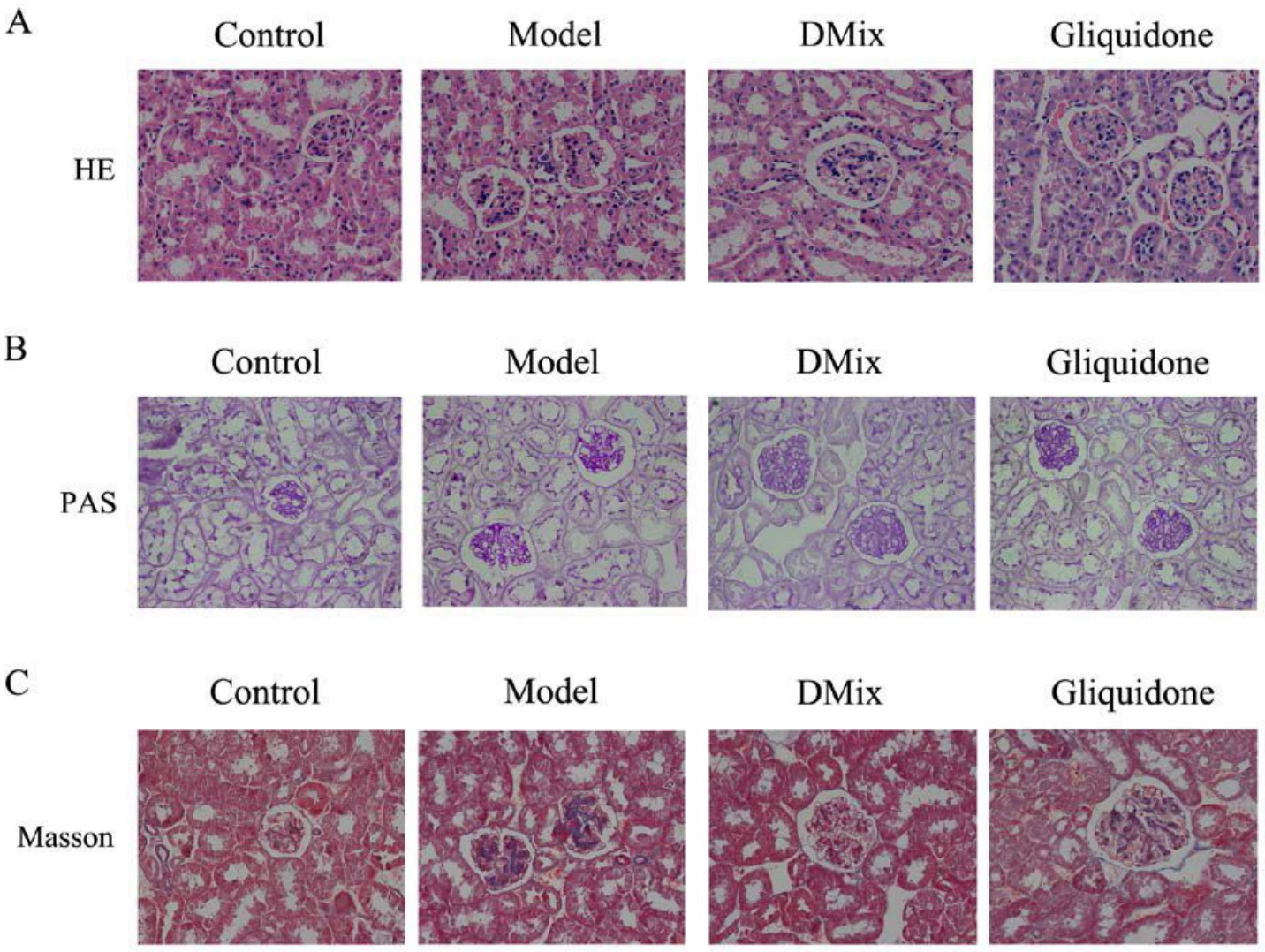

Figure 5

Photomicrographs of HE (a), PAS (b), and Masson (c) staining of mice kidneys from each group as observed under a light microscope (×400). The kidney specimen of the model group showed markedly severe destruction in glomerular and tubulointerstitial lesions, such as glomerular hypertrophy, increased mesangial matrix, interstitial cell infiltration, and collagen fiber deposition. After treatment, the overall morphology of glomerular and tubulointerstitial lesions improved significantly.

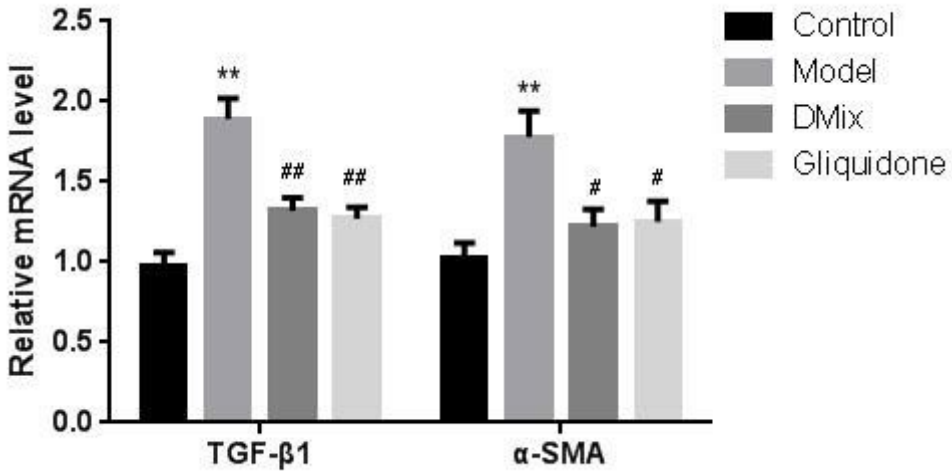

Figure 6

DMix suppressed the mRNA expression of TGF-β1 and α-SMA in mice kidneys. mRNA levels of TGF-β1 and α-SMA were determined using RT-qPCR, using β-actin as the internal standard for each sample. Data for relative quantity of TGF-β1 and α-SMA mRNA after analysis. **P<0.01 versus Control; #P<0.05 versus Model; ##P<0.01 versus Model.

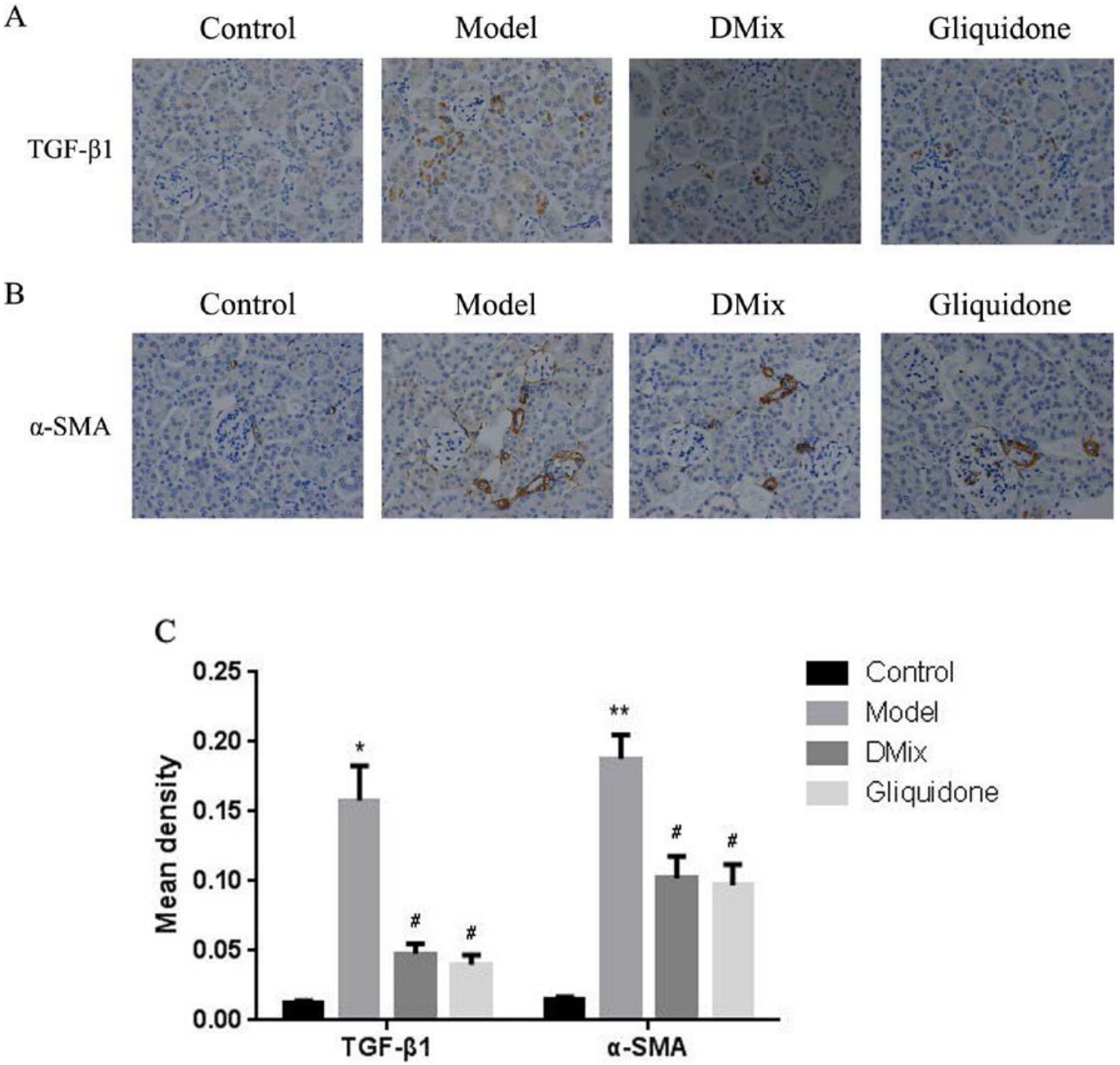

Figure 7

DMix suppressed the expression of TGF-β1 (a) and α-SMA (b) proteins in the kidney, as observed via immunohistochemical analysis under a light microscope (×400). (c) *P<0.05 versus Control; **P<0.01 versus Control; #P<0.05 versus Model.

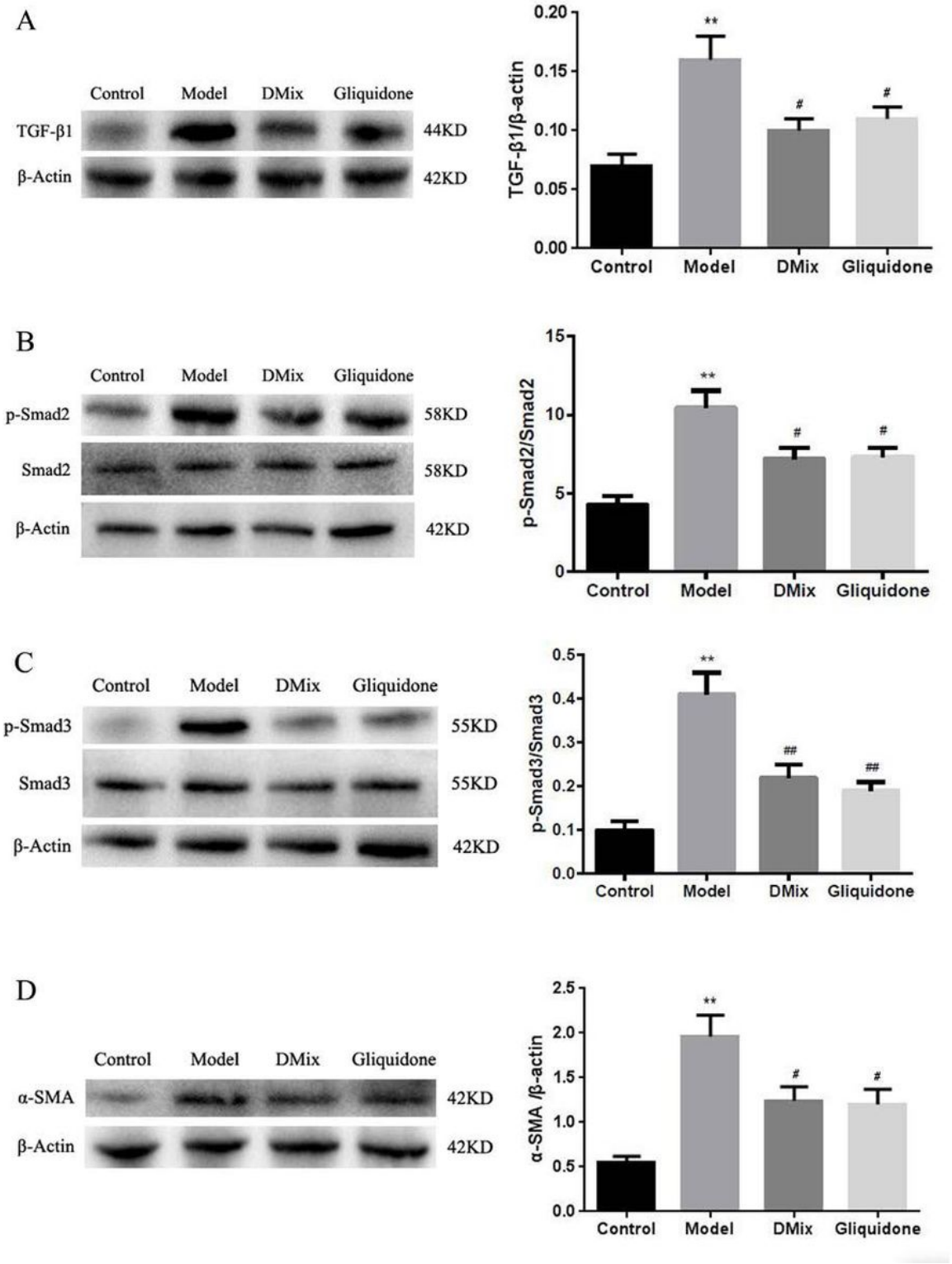

Figure 8

DMix inhibits the renal TGF-β1/Smads signaling pathway in db/db mice, as shown using western blotting. β-Actin, Smad2, and Smad3 were used as internal standards. The relative expression were the ratios of TGF-β1:β-actin (a), p-Smad2:Smad2 (b), p-Smad3:Smad3 (c), and α-SMA:β-actin (d) determined via densitometric analysis. **P<0.01 versus Control; #P<0.05 versus Model; ##P<0.01 versus Model.